Effect of Clay on Properties of Polyimide-Clay Nanocomposites

Hong-Wen Wang, Rui-Xuan Dong, Ching-Lin Liu, Hsin-Yu Chang

Department of Chemistry, Center for Nanotechnology, R&D Center for Membrane Technology, Chung-Yuan Christian University, Chung-Li 320, Taiwan, Republic of China

Received 4 April 2006; revised 16 August 2006; accepted 24 September 2006
DOI 10.1002/app.25740
Published online in Wiley InterScience (www.interscience.wiley.com).

ABSTRACT: Effect of clay on mechanical, thermal, moisture absorption, and dielectric properties of polyimide-clay nanocomposites was investigated. Nanocomposites of polyimide (ODA-BSAA) hybridized with two modified clay (PK-802 and PK-805) were synthesized for comparison. The silicate layers in the polymer matrix were intercalated/exfoliated as confirmed by wide-angle X-ray diffraction and transmission electron microscopy. Thermal stability, moisture absorption, and storage modulus for these nanocomposites are improved as hybridized clay increases. Reduced dielectric constants due to the hybridization of layered silicates are observed at frequencies of 1 kHz–1 MHz and temperatures of 35–150°C. The tetrahedrally substituted smectite (PK-805) resulted in higher mechanical strength and dielectric constants than those of octahedrally substituted smectite (PK-802), which could be attributed to their stronger ionic bonding between clay layer and polymer matrix. © 2007 Wiley Periodicals, Inc. J Appl Polym Sci 104: 318–324, 2007

Key words: polyimide; clay; nanocomposites; dielectric properties

INTRODUCTION

Polyimides (PI) have low water absorption, low thermal expansion coefficient, high thermal stability, and low dielectric constants and are widely used as high performance polymers in advanced technologies.[1–4] The study of low dielectric constant (k) of PI has been an intensive subject in recent years.[5–9] Studies on pristine and fluorinated PI have revealed the major characteristics for low dielectric constant. They are, namely, large free volume, high fluorine content, and low polarizability or symmetric fluorinated groups in the polymer structures.[5–9] However, fluorinated PI is expensive and not widely utilized. PI-layered silicates nanocomposites, formed by manipulating intercalated or exfoliated layered silicate materials (such as montmorillonite clay, MMT) within the polymer matrices, have gained intensive interests worldwide and become a potential material for microelectronic application.[10–17] The homogeneous dispersion of organically modified MMT clay in polymers would lead to enhanced thermal stability,[10–16] mechanical property,[10–13,16–17] corrosion resistance,[14] gas barrier,[12–14,17] less moisture absorption,[15,18] reduced thermal expansion coefficient,[15,17–18] and fire-retardant in the resulting nanocomposites. Dielectric studies for PI-clay nanocomposites[18–20] or PI-silica nanocomposites using silica nanoparticles[21–22] and nanotubes[23] have shown low dielectric constants close to that of pristine PI. However, the application of PI-layered silicates or PI-nano silica nanocomposites as the low k materials remains hesitated because of the suspicion of wide-ranged dielectric permittivity of smectite clay[24] and higher intrinsic dielectric properties of bulk silica (k = 3.8–4.0).[5–9] However, PI-clay nanocomposites unexpectedly show a substantial low dielectric permittivity.[18–23] Microstructures of hybridized nanocomposites are unambiguously differentiated the exfoliation structure of layered silicates from the aggregates of nanoparticles derived by sol–gel.[25] Our studies on polystyrene-clay system and PI-clay system[26–28,29] have shown that the dielectric constants of nanocomposites decrease with increasing clay contents. The reduction is attributed to the restriction of dipole orientation and confinement effect by the uniformly intercalated and exfoliated clay. In the present study, the effect of clay on the mechanical and dielectric properties of a nonfluorinated PI system is further investigated.

EXPERIMENTAL

Two purified natural smectic clays, PK802 and PK805, with a cation exchange capacity (CEC) of 116 and 98

Correspondence to: H.-W. Wang (hongwen@cycu.edu.tw).
Contract grant sponsor: National Science Council; contract grant number: NSC 92-2113M-033-008.
Contract grant sponsor: Ministry of Education, Taiwan, R.O.C.

mequiv per 100 g (mequiv/100 g), was supplied by Pai-Kong Nanotechnology company, Taiwan. PK802 is an octahedrally substituted smectite, with the chemical formula $Na_{0.89}(Al_{3.11}Mg_{0.89})(Si_8)O_{20}(OH)_4 \cdot 1.75H_2O$, and belongs to nontronite subgroup. PK805 is a tetrahedrally substituted smectite, with the chemical formula $Na_{0.75}(Fe_{0.18}Al_{3.33}Mg_{0.49})$ $(Si_{7.74}Al_{0.13}Fe_{0.13})O_{20}(OH)_4 \cdot 3H_2O$ and classified to montmorillonite subgroup.[30] A typical structure for smectic clay mineral is shown in Figure 1. The positive charge deficiency within octahedral or tetrahedral layer is compensated by cations, M^+, usually Na^+ or Ca^{2+}, residing between the layers.

[2-(Dimethylamino)ethyl] triphenylphos-phonium bromide (Aldrich, 97.0%, referred as DAETPB), and 4,4′-oxydianiline (Aldrich, 97.0%, referred as ODA), were used as intercalating agents (double swelling agents) for clays. The use of double swelling agents resulted in a better intercalation/exfoliation as explained in our previous study.[29] Briefly, DAETPB, a long-chain swelling agent, forms an ionic bond with negatively charged silicates, and ODA, a short-chain swelling agent, is available for further reaction with poly(amic acid). Monomers of ODA and 4,4′-(4,4′-isopropylidenediphenoxy) bis(phthalic anhydride) (99.0%, referred to as BSAA) were obtained from Aldrich Chemical. Solvent *N*,*N*-dimethylacetamide (DMAc, Aldrich Chemical) and hydrochloric acid (HCl, Riedel-de Haen, 37%) were used as received.

The organophilic modified clay was prepared by a cation exchange method (double swelling agents), which is a reaction between the sodium cations of layered silicates and alkyl ammonium ions of two swelling agents (or intercalating agents), as described in our previous study.[29] Before the synthesis of PI-MMT nanocomposites, the monomers of ODA and BSAA were vacuum dried at 80°C and the organophilic clay was vacuum dried at room temperature for 1 day, respectively. An appropriate amount of organophilic clay was introduced into 3 g of DMAc under magnetically stirring for 24 h at room temperature (Cup A), 1 mmol of diamine ODA was introduced into 1.5 g of DMAc under magnetically stirring 10 min at room temperature (Cup B). And Cup B was introduced into Cup A by stirring 24 h at room temperature, 1 mmol of dianhydride BSAA was introduced into 1.5 g of DMAc under magnetically stirring 10 min at room temperature (Cup C). And then, Cup C was introduced into Cup A + B by stirring 24 h at room temperature. Finally, 3 mL resultant solution was cast on a piece of glass slide (5 ×5 cm^2) and placed in a high temperature oven with a heating program as follows: 25°C → 0.5 h to 80°C → 80°C for 2 h → 2 h to 200°C, and 5 h to 300°C → 300°C for 2 h → 3 h to 25°C. The sample-coated glass substrates were then immersed into distilled water for 1 h to give the free-standing film specimens.

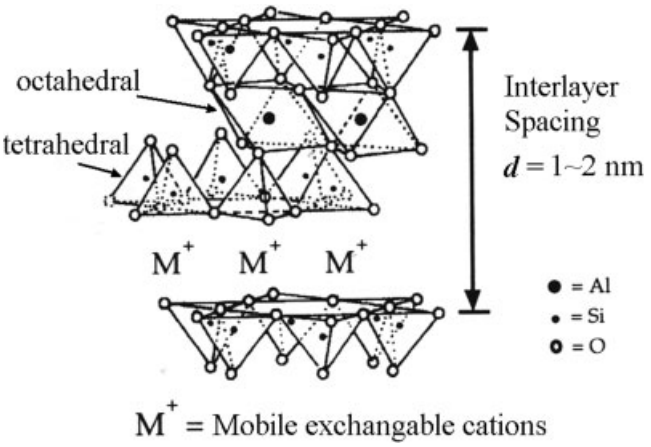

Figure 1 Typical structure of smectic clay minerals.

Wide-angle X-ray diffraction (WAXRD) study was performed on a Rigaku D/MAX-3C X-ray diffractometer with Cu target and Ni filter at a scanning rate of 2 degree/min. The samples for transmission electron microscopy (TEM) study were taken from a microtomed section of polyimide (PI)-clay nanocomposites, which were about 75 ± 15 nm thickness and mounted in a resin. A TEM (JEOL-200FX) operated at 120 kV was employed for the observation. Thermal gravimetric analysis (TGA) scans were performed using a Mettler-Toledo TGA/SDTA851 thermal analysis system in air. The scan rate was 20°C/min and the temperature ranges from 30°C to 900°C. Differential scanning calorimetry (DSC) was performed on a DuPont TAQ10 differential scanning calorimeter at a heating or cooling rate of 10°C/min in a nitrogen atmosphere from 25°C to 350°C (detect limitation −50 to 350°C). The glass-transition temperature (T_g) of PI and the synthesized nanocomposites were recorded based on the second scanning. The dynamic mechanical analysis (DMA) of the PIs and nanocomposite films were performed from 30 to 350°C (detect limitation −150 to 350°C) using a DuPont TAQ800 analyzer at a heating rate of 3°C/min and a frequency of 1 Hz. Samples for DMA tests are 6.31 ± 0.5 mm in length, 4.57 ± 0.5 mm in width, and 0.100 ± 0.005 mm in thickness. Dielectric parameters such as capacitance and dissipation factor (tan δ) were measured by an Agilent 4284A automatic component analyzer at various frequencies (1 kHz–1 MHz) under temperatures of 35–150°C (detect limitation −50 to 150°C). A vacuum evaporated gold electrode was deposited on both sides of the nanocomposite films (1.6 cm in diameter). Specimens with thickness about 100 ± 5 μm were prepared. Measurements of film thickness were carried out by using a micrometer (precision up to 0.001 mm). Five data from different areas of the specimen were taken and averaged for the calculation of dielectric constants. Films with thickness deviation less than 5% were used for dielectric characterization.

Dielectric constants (ε_r) of specimens were calculated by the equation: $C = \varepsilon_r \varepsilon_0 \frac{A}{d}$. ''$\varepsilon_0$'' is vacuum permittivity and equals to 8.85×10^{-12} F/m, ''A'' is the electrode area, and ''d'' the thickness of specimen. To exclude the effect of moisture, specimens for dielectric characterization were dried in an oven at temperature of 100°C for 2 h before measurement. To evaluate the moisture absorption of nanocomposites, the film specimens were vacuum dried at 80°C for 24 h and then weighed (W_a). The film specimens were subsequently immersed in deionized water for 24 h at room temperature for water absorption. The excess water on the surface of film specimens was wiped using a delicate-task paper wiper (Kimberly-Clark) before weighing again (W_b). Moisture absorption was calculated by using formula $(W_b - W_a)/W_a \times 100\%$.

RESULTS AND DISCUSSION

PI polymer and its nanocomposites with clay, which are synthesized using ODA, BSAA, and organophilic clay PK802 and PK805 using double intercalating agents, are formed into film specimens. To investigate the effect of clay on the properties of PI polymer, XRD, TEM, TGA/DSC, DMA, moisture absorption, and dielectric properties are evaluated.

X-ray diffraction

Figure 2 shows the XRD patterns for pristine clay, modified-clay, and their hybridized PI-clay nanocomposites (3 wt %). The d_{001} spacing of vacuum dried pristine Na^+-clay was 1.26 nm and 1.28 nm for PK-805 and PK-802 ($2\theta = 7.00^\circ$ and 6.90°), respectively. After the cation exchange, the d_{001} space increased to 1.69 nm ($2\theta = 5.19^\circ$) for PK805 and 1.80 nm ($2\theta = 4.90^\circ$) for PK802. There is lack of diffraction peak for the PI-clay nanocomposites, with 3 wt % clay, neither PK805 nor PK802. This indicates that the d spacing between the layered silicates has been either intercalated to a distance of more than 4.42 nm ($2\theta < 2.0^\circ$) or exfoliated completely in PI-layered silicate nanocomposites. XRD results imply that the clay is well dispersed or exfoliated in the PI polymer matrix. However, further evidences should be explored using TEM to reveal the exact microstructures of the nanocomposites.

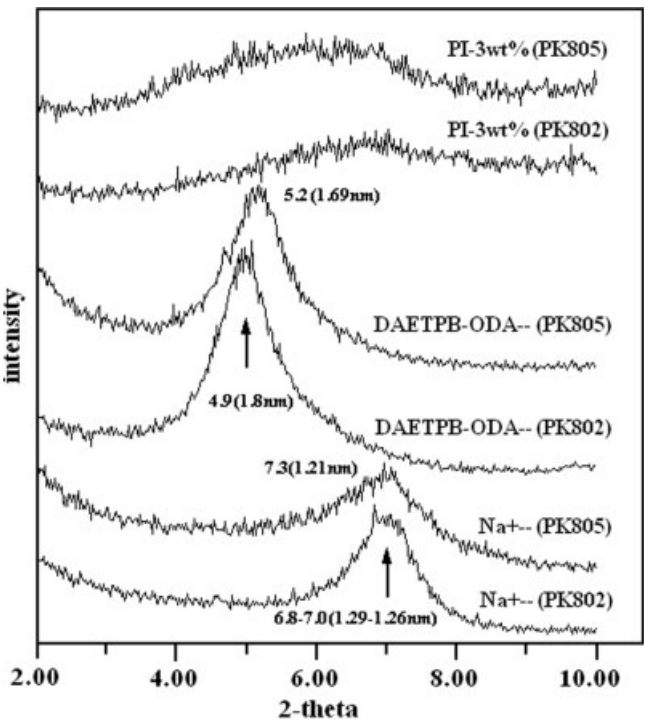

Figure 2 XRD patterns for pristine clay, modified clay, and PI-3 wt % clay nanocomposites.

TEM microstructures

Direct evidence of nanometer-scale dispersion of intercalated clay can be found in TEM, as shown in Figure 3(a,b). The number of distinguishable layered silicate particles in the 3 wt % samples shows the extent of dispersion. All nanocomposites, PI-clay (PK802 and PK805), as shown in Figure 3(a–d), exhibit well-dispersive structures. The alignment of the layered silicate platelets in one direction in some of the microstructures is most likely a result of doctoring the solutions onto the glass. In these figures, the light regions represent PI, and the dark lines correspond to the silicate layers. Individual silicate layers, along with two and three layer stacks, are exfoliating in the polymer matrix. Besides, some larger intercalated tactoids can also be identified. Nanocomposites made from ODA-BSAA with two different clay layer silicates show well dispersive and exfoliated structures, and are in agreement with the XRD characterizations.

Thermal, mechanical, and moisture absorption properties

The coefficient of thermal expansion (CTE) of PI and PI-3 wt % clay nanocomposites is shown in Figure 4, and the CTE values are summarized in Table I. PI-clay nanocomposites exhibit lower CTE than that of pristine PI, which is a general trend known from literature.[15,17–18] However, explanation of this trend is not consistent. Wei et al.[15] believed that the crystallinity of PI holds the CTE down and the CTE of crystalline PI is substantially lower than that of amorphous PI. Clay materials would reduce the CTE of PI but in different extent.[15] However, the effect of clay is not explained. Yano et al.[17] and Chang et al.[18] both attributed the low CTE of nanocomposites to the much lower CTE of clay than that of pristine PI. We believe that the Van der Waals force between polymer chains is replaced to some extent by strong ionic bonding between polymer and clay. The thermal stability of

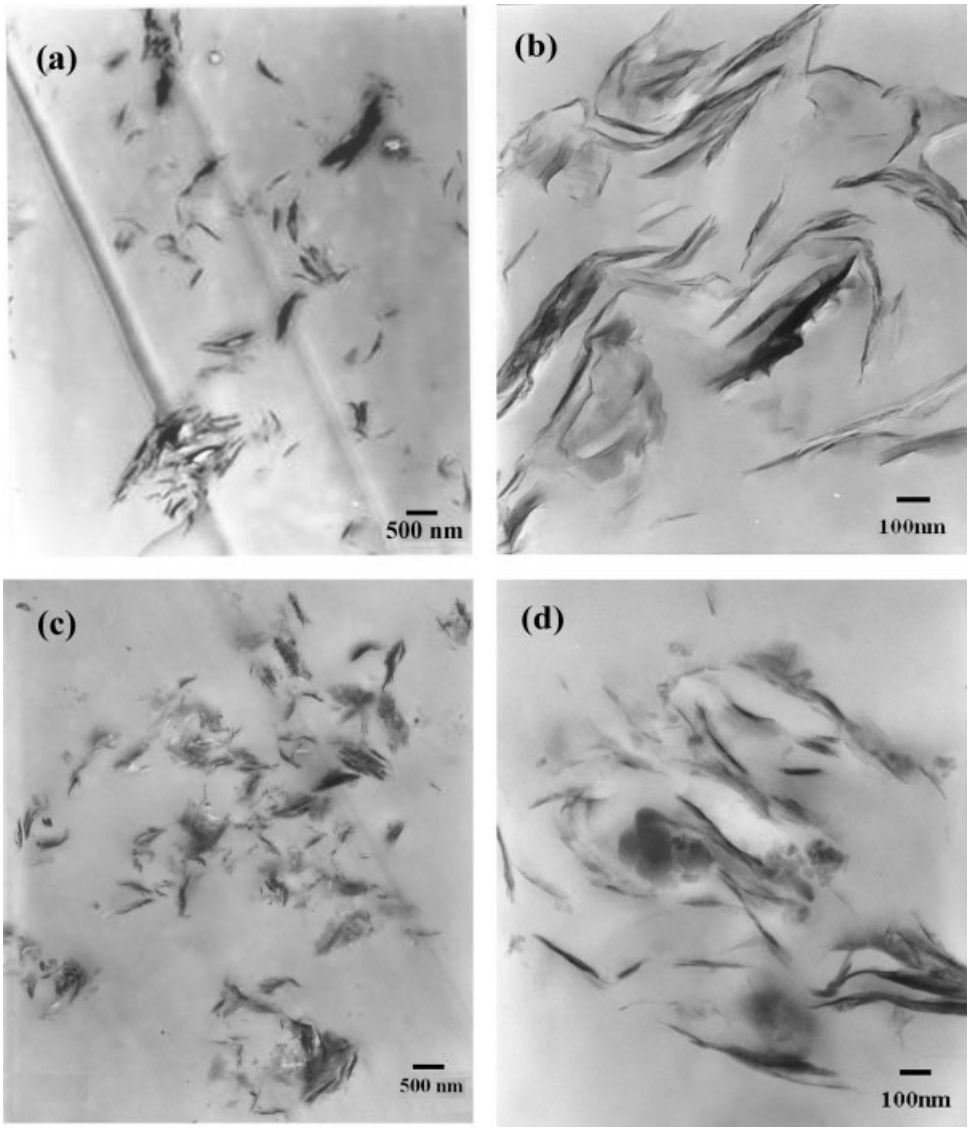

Figure 3 TEM microstructure for PI-clay 3 wt % nanocomposite, (a,b) PK-802, (c,d) PK-805.

clay greatly reduces the thermal motion of polymer chains.

The DMA for PI-clay nanocomposites of different compositions shows the storage modulus (G') of the PI-clay nanocomposites are higher than that of pristine PI, as summarized in Table I. The storage modulus of PI-clay (PK805) is higher than that of PI-clay (PK802) and much higher that of pristine PI, as depicted in Figure 5. Table I summarizes the thermal and the mechanical properties of PI and PI-clay nanocomposites. The thermal degradation temperature (T_d) and glass-transition temperature (T_g) for PI-clay nanocomposites are higher than those of pristine PI. T_d and T_g shifts toward higher temperatures as the amount of layered silicate increases. Especially, T_g obtained from DMA tan δ characterizations exhibits significant enhancement because of the PK805 incor-

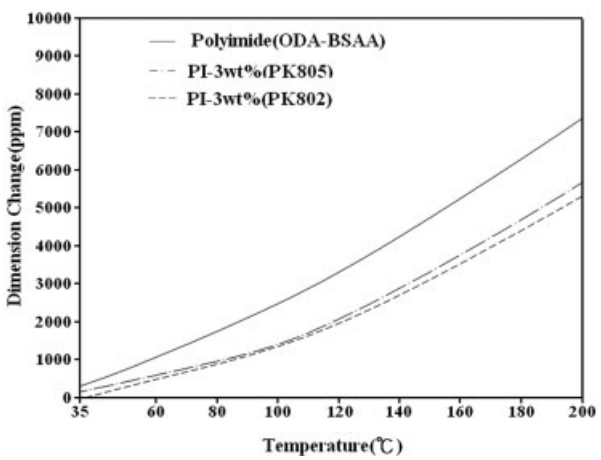

Figure 4 Thermal expansion experiments for pristine PI and its nanocomposites with PK802 and PK805.

TABLE I
Summary of Mechanical and Thermal Properties of PI-Clay Nanocomposites

	Contents of clay (wt %)	T_d(°C)[a]	T_g(°C)[b]	T_g(°C)[c] (Tan δ)	Storage modulus (MPa)	Moisture absorption (%)	CTE (ppm/°C)[d]
PI(ODA-BSAA)-clay(PK805)	0	590.75 ± 0.12	221.8 ± 0.5	245.7 ± 1.2	2006 ± 38	1.545 ± 0.002	42.74
	1	595.18 ± 0.34	224.3 ± 0.4	255.5 ± 0.8	2216 ± 10	1.420 ± 0.0015	39.73
	3	602.15 ± 0.45	229.6 ± 0.7	257.8 ± 0.5	2706 ± 25	1.315 ± 0.0021	33.41
	5	609.11 ± 0.51	231.6 ± 0.8	258.4 ± 0.3	2852 ± 48	1.199 ± 0.0032	30.16
PI(ODA-BSAA)-clay(PK802)	0	590.75 ± 0.12	221.8 ± 0.5	245.7 ± 1.2	2006 ± 38	1.545 ± 0.002	42.74
	1	594.42 ± 0.53	222.6 ± 0.3	246.7 ± 1.0	2067 ± 25	1.296 ± 0.0012	39.66
	3	599.20 ± 0.48	224.3 ± 0.4	247.9 ± 0.2	2353 ± 21	1.126 ± 0.0008	32.48
	5	607.84 ± 0.67	228.3 ± 0.6	248.5 ± 0.4	2614 ± 39	0.978 ± 0.0005	28.75

All data are obtained by averaging three samples except CTE (two samples).
[a] Thermal decomposition temperature from TGA measurement.
[b] Glass-transition temperature from DSC measurement.
[c] Glass-transition temperature from DMA measurement (30–350°C).
[d] Coefficient of thermal expansion (CTE) from TMA measurement (35–200°C).

poration, as shown in Figure 6 (b). Figure 6(a) shows that the T_g of PI-PK802 increases only slightly. The increase of T_g is tentatively attributed to the confinement of the intercalated polymer chains within the layered silicate galleries, which prevents the segmental motions of the polymer chains. As more silicate layers exfoliated in the polymer matrix, this confinement of segmental motion will be greater. The enhancement of mechanical properties by the incorporation of layered silicate clay is demonstrated. In addition, since tan δ equals G''/G', the loss modulus G'', which indicates the ability of impact absorption or energy dissipation, of PK805 is smaller than PK802 [Fig. 6(a,b)]. In these characterizations, PI-clay nanocomposites made from PK805 generally have higher mechanical and thermal stability than those made from PK802.

Moisture absorption is a critical issue for a polymer to be used in microelectronics. The moisture absorptions of PI-clay nanocomposites for different compositions are also shown in Table I. The moisture absorption of the pristine PI was 1.545%. PI-clay nanocomposite films at 5.0 wt % clay content exhibit the lowest

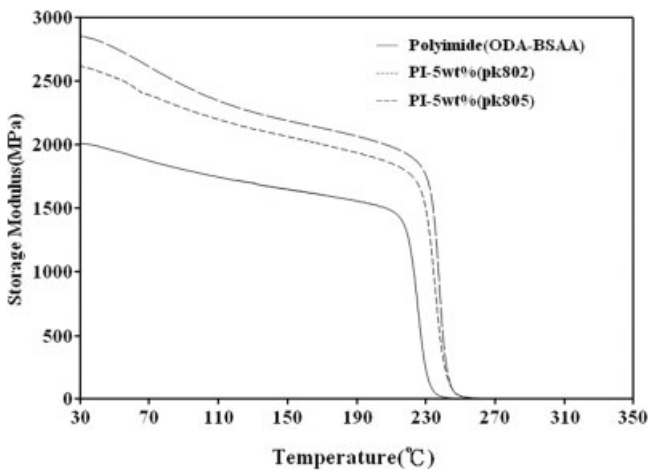

Figure 5 Storage modulus (G') for pristine PI and its nanocomposites with PK802 and PK805 from 30°C to 350°C.

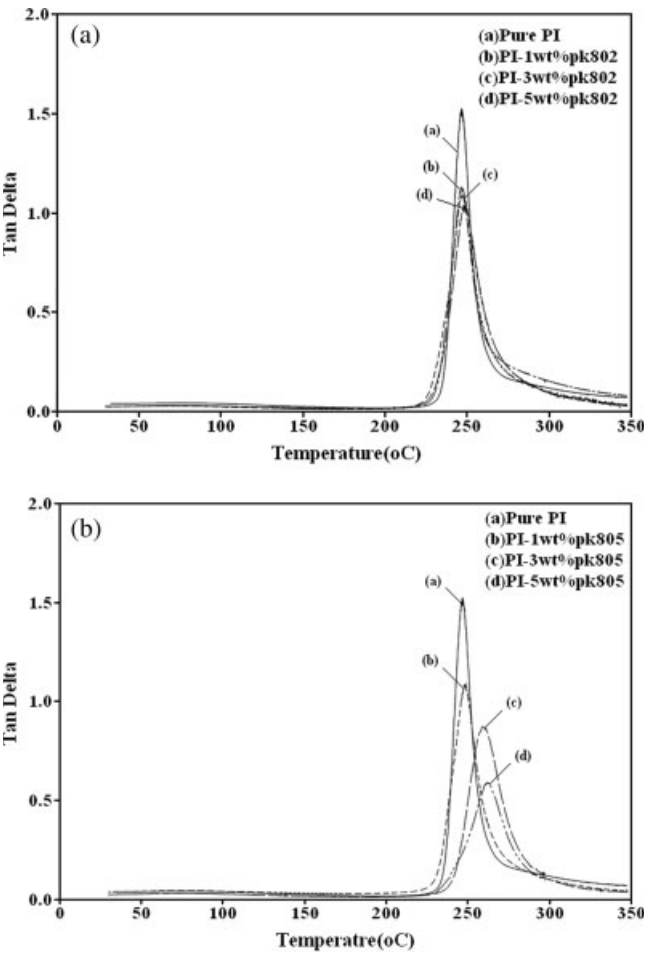

Figure 6 Tan δ (= G''/G') for (a) PI-PK802 and (b) PI-PK805 for clay content 1–3 wt %.

value of moisture absorption. PK802 exhibits slightly better performance than those of PK805. The stacked silicate sheets clearly decrease the accessibility of the polar groups of the PI and reduce the moisture absorption of nanocomposites. It is known that moisture absorption is controlled by two factors.[15] The first factor is the barrier effect of clay, which is significant because of the presence of impermeable layered silicates. The second factor is that the silicate layer is still partially hydrophilic after modification; therefore, the moisture adsorbed on silicates should be increased with the amount of silicates. These two competing effects results in a maximum reduction of moisture absorption.[15] However, in our case, the barrier effect of clay dominates at 1–5 wt % addition. The nanocomposites made from PI-clay offer this unique characteristic together with enhanced mechanical properties, which would be advantageous over other nanoporous PI materials.

Dielectric properties

Significant reduction of dielectric constants was observed for these PI-clay nanocomposites. Figure 7(a,b) shows the dielectric properties for pristine PI and PI-3 wt % clay nanocomposites at 1 kHz from 35 to 150°C. PK802 exhibits lower dielectric constant as well as lower loss than those of PK805. Figure 8(a,b) show the effect of clay loading on the dielectric constants and losses at various frequencies at 35°C for nanocomposites made from PK802 and PK805, respectively. The dielectric loss is increased because of the addition of clay as shown in Figure 8(b). It is clear that dielectric constant decreases and loss increases as loading of clay increases. Again, PK802 exhibits lower dielectric constants and slightly lower dielectric losses (before 100 kHz) than those of PK805. The dielectric constant data for the pristine PI polymer ($k = 4.6$) of present study are higher than those reported in literature. This might be due to that the purity of starting precursors used is not ultrahigh. However, the modification of dielectric constants and losses by incorporation of clay in PI are demonstrated.

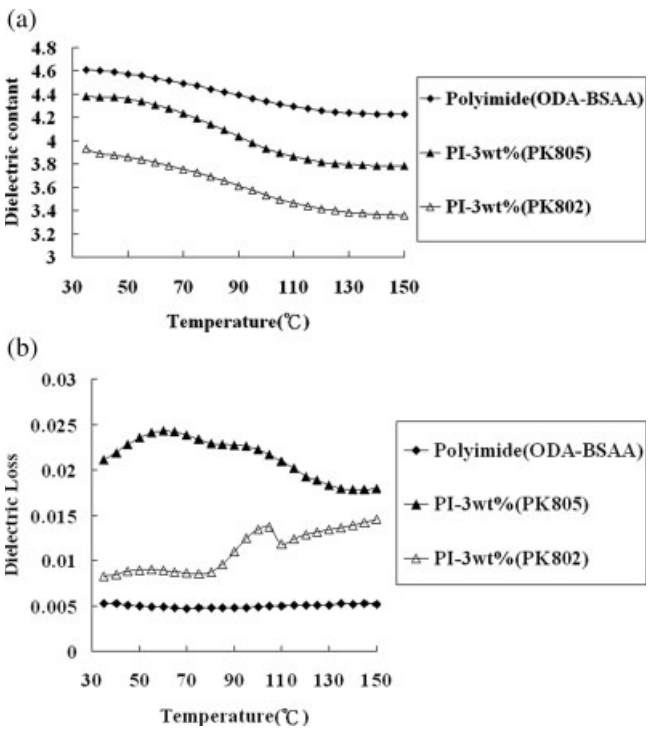

Figure 7 (a) Dielectric constant and (b) dielectric loss at 1 kHz from 35°C to 150°C.

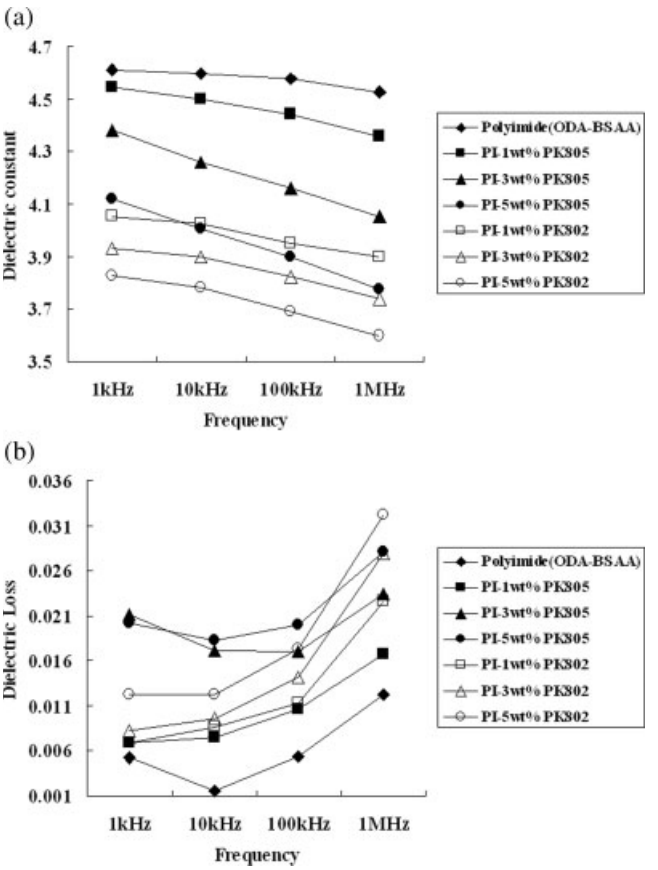

Figure 8 (a) Dielectric constant and (b) dielectric loss at 35°C from 1 kHz to 1 MHz.

It is believed that the reduced polarizability due to the nanoscopic-confinement effects in the randomly exfoliated and intercalated layer structures is largely responsible for the decrease of dielectric constants in PI-clay nanocomposites. As the content of dispersive or exfoliated layered silicates within the polymer matrix increases, the dielectric constant decreases and loss increases. The present study shows that inherent crystal defect structure of clay is also important for the dielectric properties of PI-clay nanocomposites.

PK-802 with the chemical formula $Na_{0.89}(Al_{3.11}Mg_{0.89})(Si_8)O_{20}(OH)_4 \cdot 1.75H_2O$ is an octahedral substituted clay and the negative charges are distributed in the octahedral layers. PK-805 with the chemical formula $Na_{0.75}(Fe_{0.18}Al_{3.33}Mg_{0.49})(Si_{7.74}Al_{0.13}Fe_{0.13})O_{20}(OH)_4 \cdot 3H_2O$ is a tetrahedral substituted clay and the negative charges are distributed in the tetrahedral layers. When PK-805 is intercalated in the polymer matrix, the strength of the ionic bonds between the clay layers, swelling agents, and polymers is stronger than that of PK-802 because of more direct attraction and shorter distance. The ionic attraction between intercalating agents and clay layers has been demonstrated by Pinnavaia[31] and further explored by Tsai et al.[30] and Lin et al.[32–34] The strong ionic bonding results in high mechanical, stable thermal properties, and dielectric constants. PK-802 forms weaker ionic bonds with the modifying swelling agents and polymer in the interlayer because of that the negative charges are distributed in the octahedral layers.

CONCLUSIONS

PI-clay nanocomposites fabricated using two different clays were investigated. These low cost PI-clay nanocomposites exhibit great potentials for microelectronic applications as low dielectric constant, low dielectric loss, low moisture absorption, low thermal expansion coefficient, and high mechanical strength are required. Defect structures of clay materials having significant effects on the thermal, mechanical, and dielectric properties of PI polymers are demonstrated. Octahedral substituted smectic clay PK802 exhibits weaker ionic bonding with polymer and renders the PI-PK802 nanocomposites suitable dielectric materials for microelectronics.

The financial support of grant number NSC 92-2113-M-033-008 from the National Science Council, and the Center-of-Excellence Program on Membrane Technology, the Ministry of Education, Taiwan, R.O.C., are greatly appreciated.

References

1. Lim, O. K.; Lee, J. I.; Kim, Y. J.; Park, J. Y. Microwave Opt Technol Lett 2004, 40, 177.
2. Wilson, D.; Stenzenberger, H. D.; Hergenrother, P. M. Polyimides; Chapman and Hall: New York, 1990.
3. Ghosh, M. K.; Mittal, K. L. Polyimides: Fundamentals and Applications; Marcel Dekker: New York, 1996.
4. St. Clair, A. K.; Clair, T. L.; Winfree, W. P. U.S. Pat. 5,338,826 (1994).
5. Simposon, J. O.; St. Clair, A. K. Thin Solid Films 1997, 308/309, 480.
6. Ukishima, S.; Ijijma, M.; Masatoshi, S.; Takahashi, Y.; Fukada, E. Thin Solid Films 1997, 308/309, 475.
7. Alegaonkar, P. S.; Mandale, A. B.; Sainkar, S. R.; Bhoraskar, V. N. Nucl Instrum Methods Phys Res B 2002, 194, 281.
8. Goto, K.; Akiike, T.; Inoue, Y.; Matsubara, M. Macromol Symp 2003, 199, 321.
9. Vora, R. H.; Krishnan, P. S. G.; Goh, S. H.; Chung, T. S. Adv Funct Mater 2001, 11, 361.
10. Tyan, H. L.; Leu, C. M.; Wei, K. H. Chem Mater 2001, 13, 222.
11. Tyan, H. L.; Wei, K. H.; Hsieh, T. E. J Polym Sci Part B: Polym Phys 2000, 38, 2873.
12. Chang, J. H.; Park, D. K.; Ihn, K. J. J Appl Polym Sci 2002, 84, 2294.
13. Chang, J. H.; Park, K. M.; Cho, D. H. Polym Eng Sci 2001, 41, 1514.
14. Yu, Y. H.; Yeh, J. M.; Liou, S. J.; Chang, Y. P. Acta Mater 2004, 52, 475.
15. Tyan, H. L.; Wu, C. Y.; Wei, K. H. J Appl Polym Sci 2001, 81, 1742.
16. Delozier, D. M.; Orwoll, R. A.; Cahoon, J. F.; Johnston, N. J., Jr.; Smith, J. G.; Connell, J. W. Polymer 2002, 43, 813.
17. Yano, K.; Usuki, A.; Okada, A. J Polym Sci Part A: Polym Chem 1997, 35, 2289.
18. Gu, A.; Kuo, S. W.; Chang, F. C. J Appl Polym Sci 2001, 79, 1902.
19. Jiang, L. Y.; Leu, C. M.; Wei, K. H. Adv Mater 2002, 14, 426.
20. Zhang, Y. H.; Dang, Z. M.; Fu, S. Y.; Xin, J. H.; Deng, J. G.; Wu, J. T.; Yang, S. Y.; Li, L. F.; Yan, Q. Chem Phys Lett 2005, 401, 553.
21. Yen, C. T.; Chen, W. C.; Liaw, D. J.; Lu, H. Y. Polymer 2003, 44, 7079.
22. Kramarenko, V. Y.; Shantalil, T. A.; Karpova, I. L.; Dragan, K. S.; Privalko, E. G.; Privalko, V. P.; Fragiadakis, D.; Pissis, P. Polym Adv Technol 2004, 15, 144.
23. Zhang, Y. H.; Lu, S. G.; Li, Y. Q.; Dang, Z. M.; Xin, J. H.; Fu, S. Y.; Li, G. T.; Guo, R. R.; Li, L. F. Adv Mater 2005, 17, 1056.
24. Kaviratna, P. D.; Pinnavaia, T. J.; Schroeder, P. A. J Phys Chem Solids 1996, 57, 1897.
25. Ahmad, Z.; Mark, J. E. Chem Mater 2001, 13, 3320.
26. Wang, H. W.; Chang, K. C.; Yeh, J. M.; Liou, S. J. J Appl Polym Sci 2004, 91, 1368.
27. Wang, H. W.; Chang, K. C.; Chu, H. C.; Liou, S. J.; Yeh, J. M. J Appl Polym Sci 2004, 92, 2402.
28. Wang, H. W.; Chang, K. C.; Chu, H. C. Polym Int 2005, 54, 114.
29. Wang, H. W.; Dong, R. X.; Chu, H. C.; Chang, K. C.; Lee, W. C. Mater Chem Phys 2005, 94, 42.
30. Tsai, T. Y.; Li, C. H.; Chang, C. H.; Cheng, W. H.; Hwang, C. L.; Wu, R. J. Adv Mater 2005, 17, 1769.
31. Pinnavaia, T. J. Science 1983, 220, 365.
32. Lin, J. J.; Chang, Y. C.; Cheng, I. J. Macromol Rapid Commun 2004, 25, 508.
33. Lin, J. J.; Chen, I. J.; Chou, C. C. Macromol Rapid Commun 2003, 24, 492.
34. Chou, C. C.; Chang, Y. C.; Chiang, M. L.; Lin, J. J. Macromolecules 2004, 37, 473.